Case Study

Thermal analysis of concrete bricks-embedded phase change material: A case study under hot weather conditions

Qudama Al-Yasiri [a,b,c,*], Márta Szabó [b]

[a] *Doctoral School of Mechanical Engineering, MATE, Szent István Campus, Páter K. u. 1, Gödöllő H-2100, Hungary*
[b] *Department of Building Engineering and Energetics, Institute of Technology, MATE, Szent István Campus, Páter K. u. 1, Gödöllő H-2100, Hungary*
[c] *Department of Mechanical Engineering, Faculty of Engineering, University of Misan, Al Amarah City, 62001, Iraq*

ABSTRACT

This research experimentally examines the thermal behaviour of concrete brick-based PCM layer/ capsules during severe hot summer days in southern Iraq. Three bricks were fabricated in which one brick was integrated with a PCM layer (B_L) and another integrated with PCM capsules (B_C), while the third was left bare without PCM (B_R) for comparison. The thermal performance of bricks was assessed considering the inner and outer surface temperature difference, decrement factor, time lag and average surface temperature fluctuation reduction. Besides, the mechanical strength decline of each brick was investigated to show their applicability in real constructions. Experimental results designated that B_L and B_C performed better than B_R, in which the temperature across the brick was shaved by up to 5 °C with a 30–60 min time lag. Generally, B_L exhibited slightly better thermal performance than BC; nonetheless, it showed a sharp decline in compression strength. Conclusively, the brick-based PCM layer was thermally better than that-based PCM capsules, but the latter has superior mechanical properties.

1. Introduction

In hot regions, external walls are a major source of heat gain in buildings. It was reported that nearly 33% of total heat gain was brought into the built environment through external walls in poorly insulated buildings [1]. Therefore, experts and relevant parties seek advanced technologies to reduce energy consumption by endorsing low-energy building construction materials [2]. Incorporating phase change materials (PCMs) into walls is a fast-developing technology that could enhance wall inertia and improve thermal performance [3]. The PCM can efficiently minimise the building energy by up to 18% and shift the peak load by up to 10.3 h if the PCM is incorporated well into walls considering its phase change temperature along with the best PCM quantity and position [4].

Numerous studies have recently investigated the PCM advancements in building walls as a promising solution from thermal and economic points of view [5]. Some studies have investigated the PCM as a single or separated layer integrated with insulated/non-insulated walls [6]. In contrast, others have studied the PCM integration into bricks, the worldwide popular construction element of walls [7]. For instance, Imafidon and Ting [8] numerically studied the heat flux reduction of honeycomb PCM incorporated walls for building retrofitting under weather conditions in Ottawa, Canada, concerning PCM phase transition temperature and layer thickness variation. Study outcomes indicated that the PCM of 20 °C transition temperature with 1 cm thickness performed the best under varying outdoor summer temperatures between 15 °C and 26.5 °C. Besides, the heat gain and loss of the walls

---

Nomenclature

Abbreviations

ATFR	Average temperature fluctuation reduction [°C]
B_C	Brick-integrated PCM capsules
B_L	Brick-integrated PCM layer
B_R	Brick without PCM (bare brick)
DF	Decrement factor
DSC	Differential scanning calorimeter
HCB	Hollow clay brick
PCM	Phase change material
SR	Solar radiation [W/m^2]
TGA	Thermogravimetric analysis
TL	Time lag [min]
X	Average decrease in inner surface temperature of PCM brick during the day compared with the bare brick [°C]
Y	Average increase in the inner surface temperature of PCM brick during the night compared with the bare brick [°C]

Symbols

T_i	Brick inner surface temperature [°C]
$T_{i,av}$	Brick average inner surface temperature [°C]
$T_{i,max}$	Brick maximum inner surface temperature [°C]
$T_{i,min}$	Brick minimum inner surface temperature [°C]
T_o	Brick outer surface temperature [°C]
$T_{o,av}$	Brick average outer surface temperature [°C]
$T_{o,max}$	Brick maximum outer surface temperature [°C]
$T_{o,min}$	Brick minimum outer surface temperature [°C]
$\tau_{Ti,max}$	Time at the maximum inner surface temperature of brick [min]
$\tau_{To,max}$	Time at the maximum outer surface temperature of brick [min]

were abridged by 41% and 96%, respectively. The study concluded that PCM effectiveness was restricted beyond 1 cm thickness and 20 kJ/kg.K effective heat capacity, in which no further improvement of incorporated PCM was achieved. Liu et al. [9] numerically investigated PCM-integrated lightweight building walls considering the wall's thermal resistance effect on PCM functionality and other parameters. The outcomes displayed that PCM transition temperature is more influenced by the PCM location within the wall than the wall thermal resistance. In this regard, the PCM of 22–32 °C phase change temperature in the middle of the wall showed the best performance. Besides, the study concluded that the PCM latent heat potential has more effect with low-thermal resistance walls, while high thermal resistance walls limit the PCM effectiveness. For instance, when the wall's thermal resistance increased from 2 to 5 m^2·K/W, the heat attenuation rate of the PCM wall was reduced by 2.03–4.99%, the time delay was increased by up to 1.14 h, the peak and average heat flux were reduced by 66.10–66.92% and 30.8–33.57%, respectively, compared to the wall with no PCM. Al-Absi et al. [10] experimentally examined a microencapsulated PCM into cement render and foamed concrete for the exterior finishing of walls. The results exhibited that the density and thermal conductivity of cement-based PCM decreased by 50% and 86%, respectively, compared with the pristine cement render. In addition, the incorporated PCM has increased the cement render thermal energy storage by 38 J/g, improving its thermal mass. However, the study highlighted that the compressive strength was decreased by 53% for the PCM-integrated cement render but increased when foamed concrete was integrated by up to 28%– 49.7% due to filling concrete air gaps. Arıcı et a. [11] studied the energy-saving potential and thermal comfort of dividing the PCM into two while controlling their melting temperature and position. The study aimed to evaluate the annual energy-saving and indoor temperature stability under climate conditions of Kocaeli province, Turkey. Seven cases were investigated, employing one/two PCM layers applied at the inner, outer, or wall sides. Study findings discovered that the best PCM transition temperature was varied between 5 °C and 30 °C. In addition, two PCMs, one with a 17 °C phase change temperature at the wall outside and the other with a 25 °C melting temperature at the inside, have increased the annual energy saving by 17.2%, compared with 16.8% for a single PCM layer. Shaik et al. [12] investigated the potential of five PCMs with different melting temperatures (specifically OM18, OM21, OM29 and two form-stable PCMs) to save air-conditioning costs and mitigate CO_2 emissions when integrated with clay bricks at different climates. The study looked at six PCM places in bricks: the exterior side, the middle, the inner side, the outer and middle sides, the middle, inner sides, and the outer and middle sides. The findings revealed that the greatest annual energy cost saving was obtained for the OM29 PCM layer positioned at the outer side of the brick, reaching $2079 and $2095 in hot-arid and composite climates, respectively. According to the study, the largest CO_2 emissions reduced were 87.80 tonnes of CO_2 per year in hot-arid climates and 88.42 ton-CO_2 per year in composite climates, with payback periods of 11.29 and 11.21 years, respectively.

Literature studies have reported that PCM-integrated bricks could shrink surface temperature by up to 6 °C and reduce heat transfer by up to 30% [13]. However, reports have shown that the PCM would influence the mechanical strength of walls when combined into a microencapsulation method [14]. Therefore, careful integration of PCMs into bricks is required to gain their advantages with minimal

negative effects. Several research works have studied PCMs incorporated constructive bricks at different hot locations. Among recent investigations in Moroccan weather conditions, Mahdaoui et al. [15] quantitatively explored the heat transfer and temperature fluctuation reduction of PCM capsules paired with hollow bricks. The study proposed different PCM amounts out of brick volume, specifically 6%, 10%, 16% and 20%. The outcomes revealed that the thermal performance of the brick was enhanced as the PCM amount increased. The best performance was attained at 16% and 20%. Besides, the inner surface temperature of the PCM wall was stabilised more than the reference wall with notable time shifting, which eventually could enhance thermal comfort and decrease the energy consumed for air-conditioning systems. Elmarghany et al. [15] studied several PCM types of configurations-filled common blocks for a one-year energy-saving analysis. The study investigated vertical and horizontal PCM elements to quantify the best orientation for PCM utilisation. The results indicated that the thermal characteristics of PCM-filled blocks were enhanced by improving their thermal storage ability and shrinking and shifting peak load. *n*-Eicosane outperformed the other PCM types, lowering the maximum temperature to 37.86 °C and decreasing and shifting the peak heat flux by 29% and 9.28%, respectively. Furthermore, the study found that the average inner surface temperature was reduced by 1.5%, with an 8% reduction in total energy transfer. The *n-Eicosane* saved energy by 18.69% compared to other PCM types, while P116 resulted lowest saving by 0.71%. The study concluded that the PCM was more effective in the horizontal elements (i.e., roofs) more than the walls. Under the Marmara climate, Turkey, Tunçbilek et al. [16] explored the finest hollow brick/PCM combination considering their seasonal and annual thermal performance. The optimal transition temperature, PCM amount and position were studied and compared against bare bricks of air gaps. The study outcomes showed that the optimal transition temperature of PCM was associated with the season. However, the optimal PCM melting temperature for the location under study was 18 °C, in which the thermal performance of modified bricks was improved by 17.6% annually. The study further concluded that the PCM was effective during all seasons, and its thermal performance could be maximised with the proper selection of PCM fusion temperature along with the best quantity and position. Said Hamdaoui et al. [18] used Fluent software-based finite volume analysis and enthalpy-porosity methods to numerically investigate the integration of microencapsulated PCM into the solid part of hollow clay bricks (HCB). They tested several bricks with varying air gaps (specifically three, six, eight, and twelve, denoted as HCB-3, HCB-6, HCB-8, and HCB-12, respectively), and their thermal properties were evaluated. The study findings revealed that the thermal behaviour of the investigated HCBs differed, with the thermal reaction time lags of HCB-3, HCB-6, HCB-8, and HCB-12 being 1 h, 1 h and 43 min, 2 h and 27 min, and 4 h, respectively. Furthermore, the investigation found that HCB-3's thermal behaviour was identical to that of HCB-6, while HCB-8's thermal reaction was equivalent to that of HCB-12. As a result, instead of HCB-12 (15 cm thickness), outside walls might be built with HCB-8 (10 cm thickness), and HCB-3 (5 cm thickness) could be used instead of HCB-6 (7 cm thickness). The study also concluded that PCM integration considerably reduced brick volume, with HCB volume lowered by up to 30% when compared to pure brick. Ru et al. [17] modified two types of shape-stabilised PCM-based brick made of recycled aggregate pavement, namely PEG-400/SiO$_2$ composite and Tet/SiO$_2$ composite. Both brick types were tested considering thermal and mechanical methods, including Scanning electron microscopy (SEM), Differential scanning calorimeter (DSC) and Thermogravimetric analysis (TGA) tests. Findings revealed that SiO$_2$ successfully adsorbed the PCMs, and the PEG-400/SiO$_2$ was superior to Tet/SiO$_2$. Considering the thermal stability over cycles, the TGA test indicated that both composite PCMs had good physio-chemical properties throughout the test temperature range. Furthermore, mechanical tests revealed that Tet/SiO$_2$ PCM brick
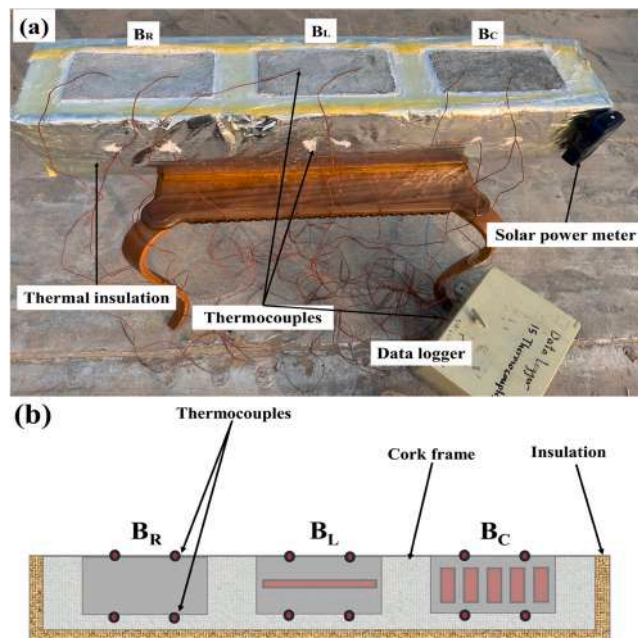

Fig. 1. Experimental set-up (a) in-site rig, (b) schematic side view showing the position of the thermocouple on the surfaces of reference brick (B$_R$), PCM-layer brick (B$_L$), and PCM-capsules brick (B$_C$).

showed higher compressive strength and flexural strength than the PEG-400/SiO$_2$ PCM brick. However, results indicated that 60% recycled aggregate content with 5% shape-stabilised PCM at 28-day strength was higher than that of 70% recycled aggregate with 10% PCM content. The study concluded that the Tet/SiO$_2$ composite brick was better than PEG-400/SiO$_2$ as a PCM from the thermal and mechanical aspects, but it has an economic concerns due to increased price of composite-shape material preparation.

According to the literature analysis, numerical studies have mostly investigated integrating PCM into building walls as a layer to simplify physical models, regardless of its applicability in real constructions. These studies have overlooked the effect of PCM encapsulation to avoid leakage, which eventually impacts the thermal behaviour of walls [18]. Besides, experimental studies did not quantify the applicability of bricks-based PCM capsules and the declination in their mechanical properties compared with the bricks-based layer PCM. Therefore, this study aims to analyse the PCM experimentally macroencapsulated into capsules and equivalent layer incorporated inside concrete bricks from the thermal and mechanical viewpoints. This work is believed to provide answers regarding the applicability of bricks-based PCM and their thermal and technical issues towards adopting the best incorporation techniques of PCM within building structures.

2. Materials and methods

2.1. Experimental set-up

Three concrete bricks were designed, fabricated and examined under severe hot summer conditions in Al Amarah city (Latitude: 31.84° & Longitude: 47.14°), Iraq. Two bricks were integrated with PCM in which, one integrated with PCM capsules (B$_C$), one with PCM layer (B$_L$), and the third left without PCM for comparison (B$_R$). In order to create an isolated space from the hot weather conditions, a box of 1000 × 200 × 160 mm (length × width × thickness) was prepared to hold the tested bricks and separate the outer and inner surfaces, as shown in Fig. 1. The box was made from a dense cork (straibor boards) of high insulation nature and covered with fibreglass insulation. The examined bricks were placed inside the cork frame after careful insulation using high-quality silicon foam from inside and outside to minimise heat losses between the inner surface of the bricks and the outdoor ambient.

2.2. PCM concrete bricks

Concrete brick is a popular brick type worldwide for wall construction. In Iraq, they have been used for walls and fence installations for decades, especially for low-income inhabitants, thanks to their excellent mechanical strength and low cost. However, concrete bricks have poor thermal performance compared with other types, such as fired-clay bricks, limiting their use in residential building constructions [19]. The studied concrete bricks in this research have dimensions of 230 × 120 × 70 cm (length × width × depth), which is a popular size in the country for constructive bricks. The concrete mixture was made of cement, sand and gravel mixed with a ratio of 1:1.5:3, according to the Iraqi insulation blog, to prepare low-density concrete blocks [20].

As mentioned previously, two bricks were integrated with PCM macroencapsulated inside containers (capsules and layer) and immersed during bricks preparation. For this purpose, locally available aluminium was used for macroencapsulation thanks to its high thermal conductivity to enhance the PCM thermal performance and compatibility with PCM and concrete. The rectangular-shaped containers were formed in a way to hold the same quantity of PCM (~145 g) in each PCM brick, immersed at the centre of the bricks to preserve their mechanical properties. Table 1 lists the design specifications of PCM containers, and Fig. 2 views the test bricks.

The PCM used in this research is an Iraqi petroleum paraffin wax, locally formed in huge amounts in governmental refineries as a waste product. This product has several favourite characteristics for thermal energy storage, such as high storage capacity, a high melting temperature within the site temperature variation, and stability after several cycles [21]. Table 2 lists the main characteristics of paraffin wax [22], whereas Fig. 3 shows some photos of PCM brick preparation.

2.3. Measurements

Thermocouples (sensors) attached to a multi-channel Arduino (type Mega 2560)-based data logger were employed to measure the outer and inner surface temperatures of tested concrete bricks and ambient temperature. In this regard, two sensors were attached to the outer brick surface; two were fixed on the inner surface to measure the average temperature variations. Besides, another two thermocouples were positioned outside the experimental rig with a suitable position to record the average ambient temperature during the experiment period. All thermocouples recorded temperature with 30 min time step to track the temperature variation during the day and night hours and continuously stored in storage memory attached to the Arduino. On the other hand, the solar radiation variation of each experimental day hours was recorded by a solar power meter with 30 min time step. Besides, a thermal imaging camera was used to show the temperature behaviour of bricks' outer surface temperature for one day at four different times,

Table 1
Design specifications of macroencapsulation containers.

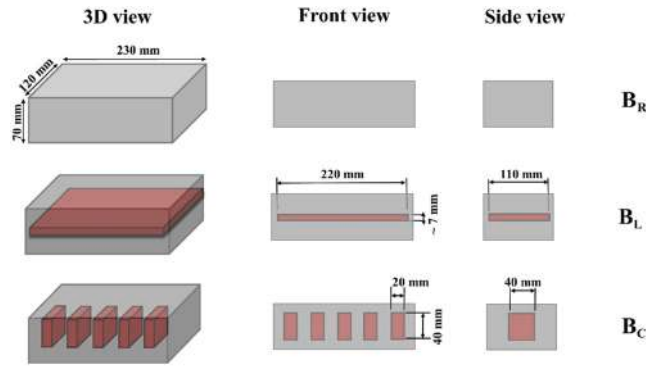| Brick sample	Container configuration	PCM container dimensions (mm)	No. of containers
B$_R$	————	————	————
B$_L$	Rectangular panel	220 × 110 × ~7	1
B$_C$	Rectangular capsules	40 × 40 × 20	5

Fig. 2. View of tested concrete bricks.

Table 2
Main characteristics of paraffin wax (PCM).

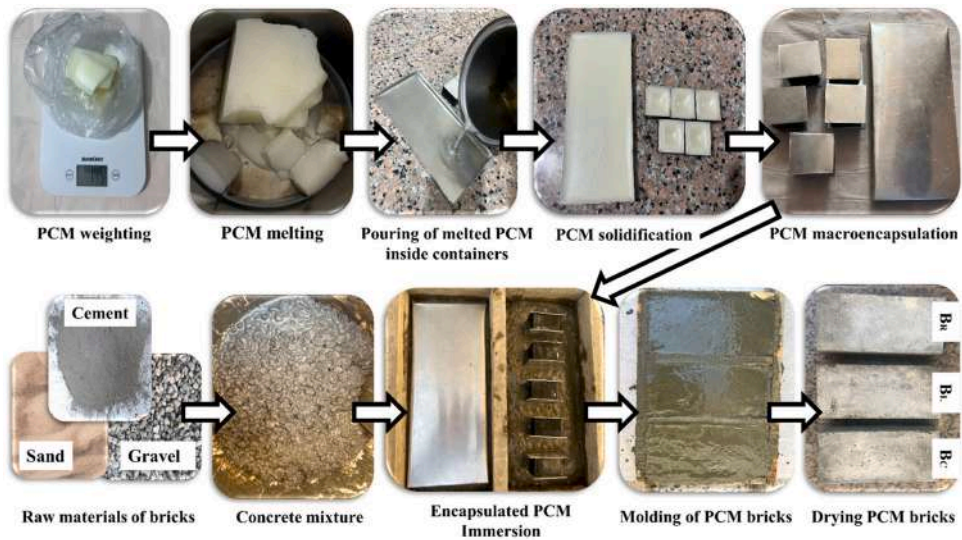| Characteristics/ Properties	Value/Property
Form	Whitish jelly
Transition temperature (°C)	40–44
Thermal conductivity (W/m.K)	0.21
Density (kg/m^3)	930 (solid)830 (liquid)
Latent heat of fusion (kJ/kg)	190
Specific heat (kJ/kg.K)	2.1

Fig. 3. Fabrication of PCM bricks.

specifically at 6:00, 12:00, 18:00 and 00:00. The camera work based on infrared thermography, which has a good inspection potential to compare among tested bricks [23]. The detailed specifications of the used instruments/devices are listed in Table 3.

2.4. Performance analysis of tested bricks

Various thermal indicators have been analysed in the current work to compare the thermal behaviour of tested bricks. These comparison indicators included the average temperature difference between the inner and outer brick surfaces, the decrement factor, the time lag and the average temperature fluctuation reduction, as follows:

2.4.1. Surface temperature reduction
The benefits of using PCM in this work were estimated as the difference between the bricks' outer and inner surface temperatures (i.

Table 3
Specifications of measurement devices used in the experiment as presented in the manufacturer's technical data sheet.

Instrument	Thermocouples (0.2 mm)	Solar power meter	Thermal imaging camera
Model	T-type	SM206	WB-80VOLTCRAFT®
Manufacturer	TEMPSENS (India)	BESTONE INDUSTRIAL Ltd. (China)	VOLTCRAFT® (Germany)
Range	-270–370 °C	0.1–399.9 W/m^2	-20–600 °C
Resolution	————————————	0.1 W/m^2	$\leq$ 254
Accuracy	+ /- 0.5 °C	$\pm$ 10 W/m^2	$\pm$ 2% $\pm$ 2 °C (tested @25 °C)
Photo of the device			

e., T_o and T_i) at each time of thermal cycles. The temperature difference between T_i and T_o indicates how high the surface temperature reduction of each brick side was.

2.4.2. Decrement factor

The decrement factor (DF) refers to the temperature decrement across the brick, considering the maximum and minimum marks of inner and outer surfaces. This indicates how high the cyclic reduction of temperature is across the brick, where the low DF value means better thermal management in the brick. Mathematically, the DF could be calculated by Eq. (1) as follows:

$$\text{DF} = \frac{T_{i,\max} - T_{i,\min}}{T_{o,\max} - T_{o,\min}} \tag{1}$$

2.4.3. Time lag

The time lag (TL) earned from incorporating PCM into bricks is another important indicator since it shows the ability of PCM (as a dynamic insulator) to resist the heat flow and shift it from peak time to off time. In other words, the time difference between the highest inner and outside surface temperatures of brick may be used to evaluate this indication., according to Eq. (2) [24], as follows:

$$\text{TL} = \tau_{T_{i,\max}} - \tau_{T_{o,\max}} \tag{2}$$

where $\tau_{Ti,max}$ and $\tau_{To,max}$ refer to the time at the maximum surface temperature of the inner and outer brick surfaces.

2.4.4. Average temperature fluctuation reduction

The average temperature fluctuation reduction (ATFR) in the inner surface of bricks can be studied, considering the average inner surface temperatures throughout the day and night, not only the maximum and minimum temperatures as in the case of DF. This may provide a better understanding of how the temperature of PCM-based bricks was lowered when compared to bare bricks throughout the thermal cycle. ATFR could be calculated by combining the average decrease in the inner surface temperature of a PCM brick during the day (compared to the reference brick, denoted as X) with the average increase in the inner surface temperature of the PCM brick throughout the night (denoted as Y). The daytime was considered from 6:00–18:00, while the nighttime started after 18:00 till the beginning of the next thermal cycle at 6:00. Accordingly, the ATFR value of B_L and B_C compared with B_R could be estimated each day according to Eqs. (3)–(5) [25].

$$\text{ATFR} = \text{average (X)} + \text{average (Y)} \tag{3}$$

$$\text{X} = T_{i,no\ PCM} - T_{i,PCM} \tag{4}$$

$$\text{Y} = T_{i,PCM} - T_{i,no\ PCM} \tag{5}$$

where $T_{i,no\ PCM}$ and $T_{i,PCM}$ are the inner surface temperature of the bare brick (B_R) and PCM bricks (B_L and B_C), respectively.

In addition to the thermal performance indicators, the mechanical properties of tested bricks will be examined in terms of crushing test to quantify the decline in bricks' mechanical strength.

2.5. Statistical analysis

Statistical analysis was verified to determine the effects and significance of the evaluated variables in the study. The one-sample t-Test analysis (hypothesis testing) was conducted using OriginPro software on the inner surface temperature of tested bricks. This statistical test could show the difference between the PCM bricks and the bare brick.

3. Results

The current work was conducted under weather conditions in Al Amarah, southern Iraq, for three sequential summer days from 09 to 11/09/2022. The climate of this city is characterised as tropical and subtropical desert climate according to the Köppen climate classification, where the ambient temperature reached the mark of 51.1 °C in July 2022 [26]. The thermal map showing the average hourly ambient temperature of the study location for the current year is indicated in Fig. 4. The figure shows that September is characterised by high ambient temperatures starting from the early day hours encountered with high incident solar radiation, particularly at noon.

3.1. Surface temperature variation

Fig. 5 shows the temperature variation of tested bricks in terms of each brick's average inner and outer surface temperatures against the ambient temperature and SR during the three thermal cycles.

As could be observed from the figure above, the first day experienced high SR and ambient temperature more than the following two days, exceeding the mark of 1100 W/m^2 and 51 °C, respectively, at noon. However, the ambient temperature endures the mark of 35 °C in the late time of the day and beginning hours of the following day. The second and third days of the experiment experienced lower SR and ambient temperature with a daily temperature difference of about 15 °C (the variation in temperature between the highest and lowest temperatures). In accordance with these trends, the outer surface temperature (T_o) of bricks increased gradually as the SR and ambient temperature increased, reaching the highest temperatures between 13:00 and 14:00 each day. The inner surface temperature (T_i) of bricks, from the other side, showed a similar trend with an obvious time lag. Fig. 6 shows some thermal images for the outer surface temperature of tested bricks during the second day of the experiment at different times.

The thermal images indicated that the outer surface temperature of bricks was almost the same in the early morning hours (at 6:00) when the ambient temperature was low. The outer surface temperature of each brick was different at midday (at 12:00), indicating high outer surface temperatures of PCM-integrated bricks (B_C in particular) compared to the bare one. During this time, the PCM melting is guaranteed, and the heat is charged into the PCM placed at the centre of PCM bricks, resulting in lower inner surface temperatures. At 18:00, the outer surface temperatures of PCM-integrated bricks were slightly higher than that of the reference brick due to discharged heat during solidification. Besides, the surface temperature was nearly the same at midnight (at 00:00), and the bricks had a relatively similar temperature after the completed solidification of PCM.

3.2. Temperature difference, DF, TL and ATFR

Diminishing the inner surface temperature is the supreme objective of incorporating PCM into building elements [28]. Fig. 7 shows
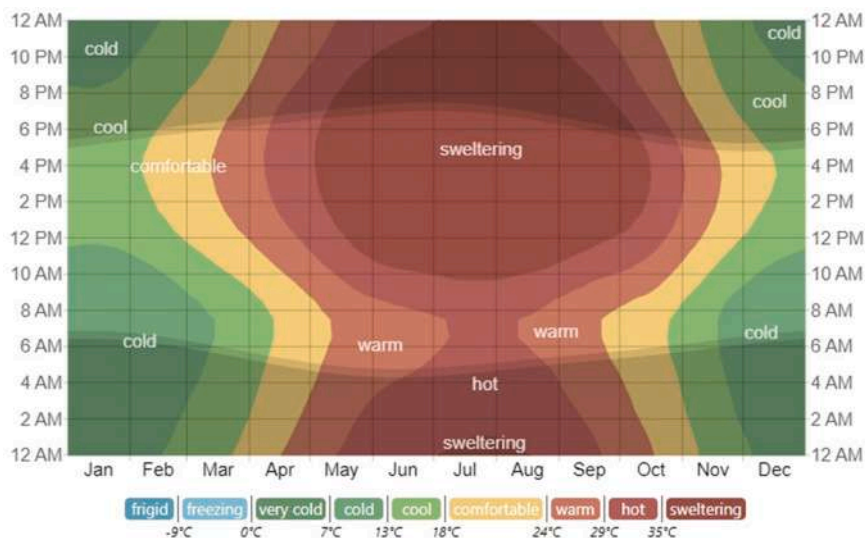

Fig. 4. Average hourly ambient temperature of Al Amarah city, 2022 [27].
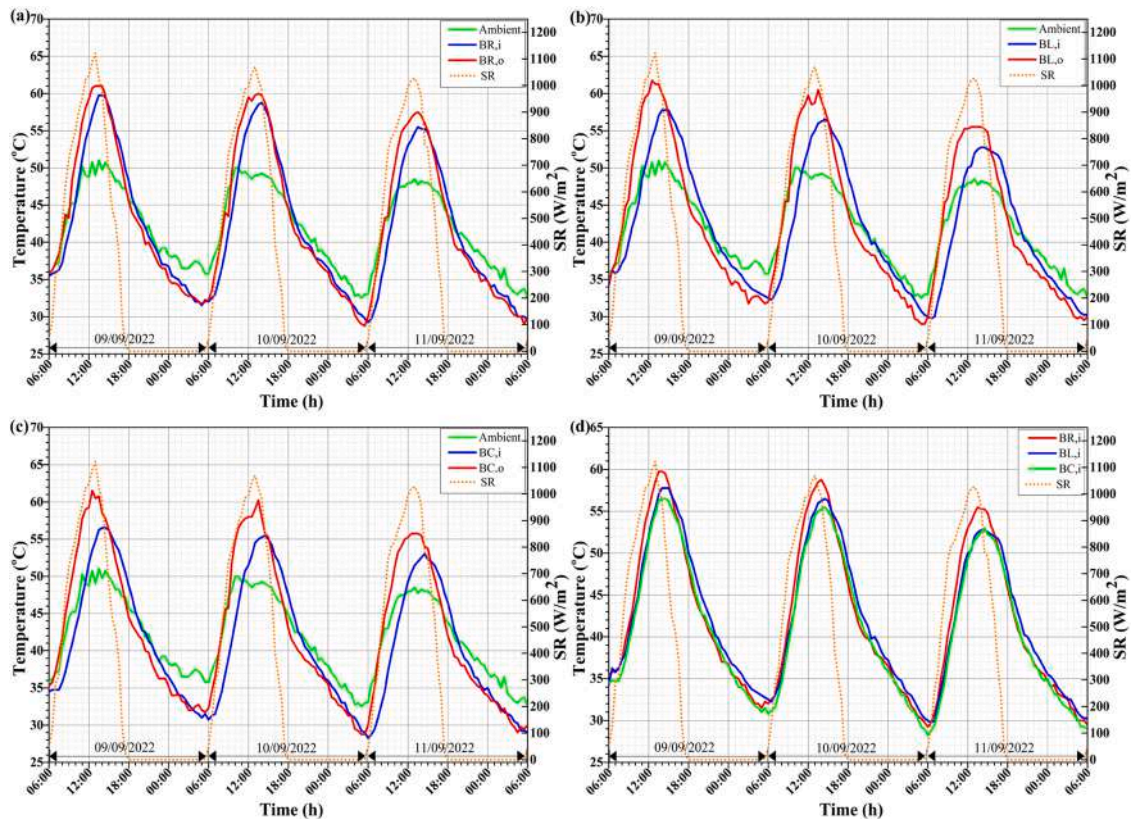
Fig. 5. (a) reference brick (B_R) vs ambient temperature and solar radiation (SR), (b) PCM-layer brick (B_L) vs ambient temperature and SR, (c) PCM-capsules brick (B_C) vs ambient temperature and SR, (d) average inner surface temperature (T_i) for B_R, B_L and B_C vs SR.

the variation of temperature difference during full-day cycles.

As clearly designated in Fig. 7, PCM-integrated bricks showed a higher temperature difference than the bare brick, reaching a maximum mark of 11 °C against 6 °C in the best case. B_L and B_C showed similar temperature differences during day hours; then, the difference fluctuated after 18:00. The figure also shows that the temperature difference of B_R after this time (i.e., from 18:00 till the beginning of the next cycle) was bigger than the case of B_L and B_C since the concrete was releasing stored heat (in B_R) faster than the composite concrete (PCM/concrete), as the ambient temperature drops in this period. However, the temperature difference in the day hours from 6:00–18:00 is the most important for evaluation since it impacts the energy performance of bricks during peak hours. The reversed temperature behaviour of PCM bricks (i.e., B_L and B_C) during the night has a negative impact on the thermal comfort of buildings, especially residential buildings, due to the PCM solidification phase. This issue is common in passive PCM incorporation applications and could be solved by employing the potential of night ventilation, as discussed in different research studies [29,30].

The DF, as earlier defined, displays the temperature fluctuation damping due to PCM incorporation. Fig. 8 displays the results of DF for tested bricks over thermal cycles.

In general, PCM-integrated bricks designated better DF than the bare brick. However, B_L showed slightly better performance than B_C in all cycles. B_L showed DF over the B_R by 0.133, 0.094 and 0.038 in the three cycles, whereas B_C showed 0.109, 0.087 and 0.017, respectively. Compared with B_R, B_L showed improvement by 13.77%, 10.13% and 4.21% in the 1st, 2nd and 3rd cycle, while B_C improved by 11.28%, 9.38% and 1.88%, respectively. These results indicated noteworthy enhancement in the PCM bricks compared with the reference bare brick, showing better thermal resistance of the PCM bricks. The thermal resistance slightly differed between the brick-based PCM layer and that-based PCM capsules.

In the open literature, researchers often study the DF along with the TL to quantity the thermal resistance enhancement of PCM elements [24,31]. These two indicators give a powerful clue about the advantages of PCM incorporation within the bricks. The calculation results of TL for the tested bricks are presented in Fig. 9.

As stated before, the TL indicates how long PCM-integrated bricks can shift the peak temperature compared with bare brick. In this regard, Fig. 9 clearly shows that B_L and B_C had better TL than B_R, considering the highest inner and outer temperatures of the brick. Generally, B_L and B_C showed similar TL in all cycles, resulting from a similar time of highest outer and inner surface temperatures. The TL in the B_R ranged between 30 and 60 min against 60–90 min in B_L and B_C, indicating temperature time shifting of 30–60 min more than the bare brick.

In addition to the DF and TL, the ATFR results present the temperature stability of the PCM bricks' inner surfaces compared with the
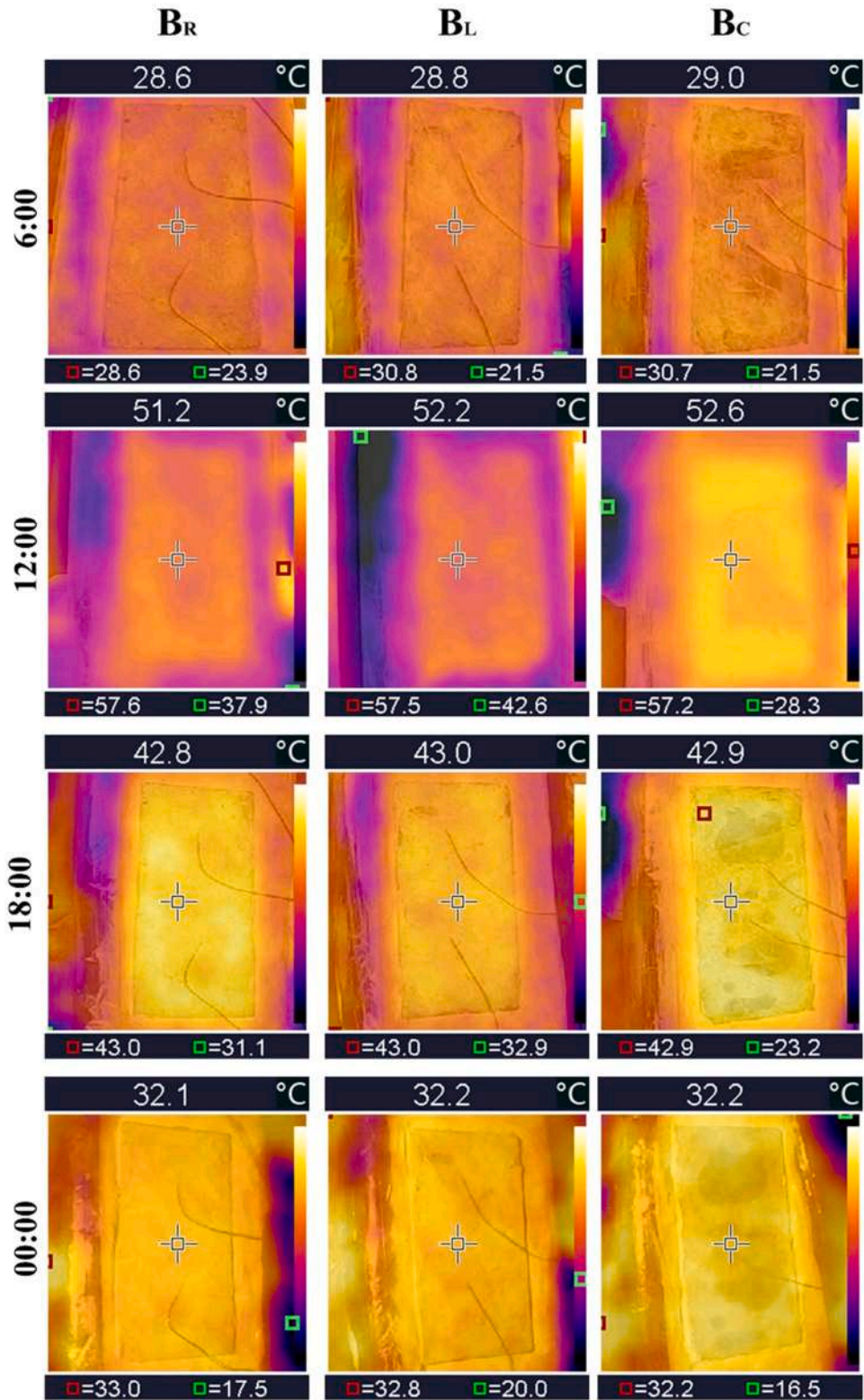
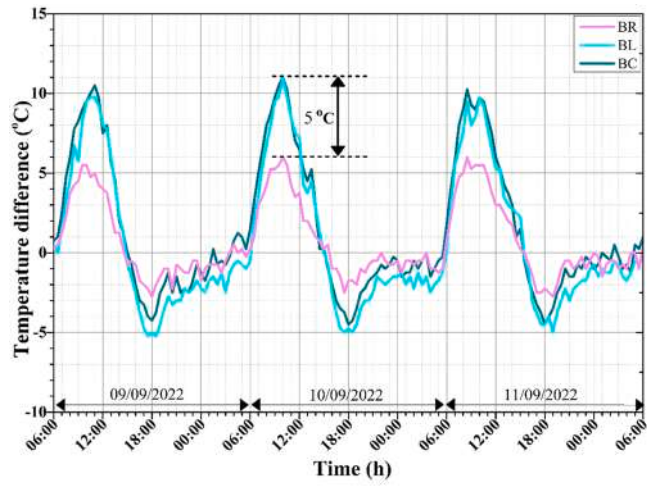**Fig. 6.** Thermal images for tested bricks at different times on 10/09/2022.

Fig. 7. Temperature difference variation of tested bricks.
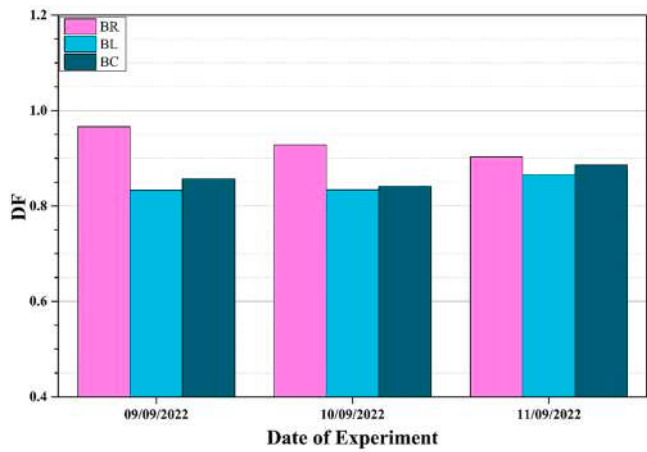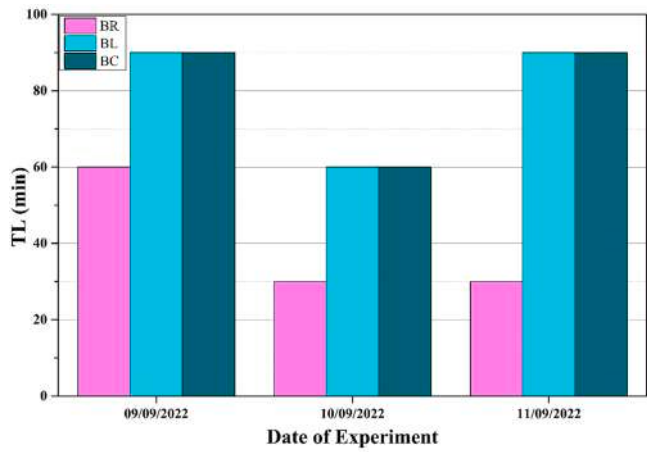

Fig. 8. DF of tested bricks.
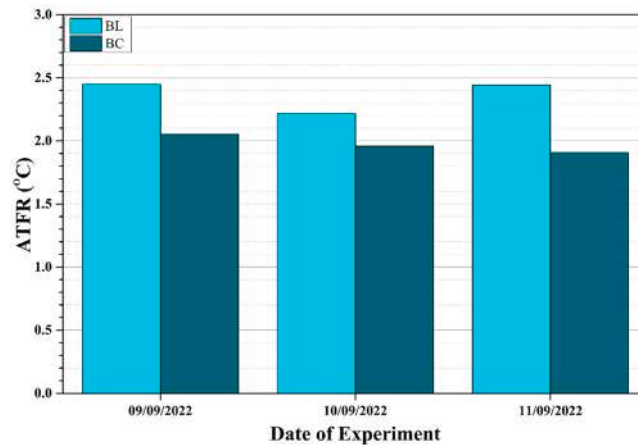

Fig. 9. TL of tested bricks.

Fig. 10. ATFR of PCM-integrated bricks.

bare brick throughout the thermal cycle. In this regard, Fig. 10 shows the calculated AFTR for B_L and B_C compared with B_R.

B_L showed better ATFR than B_C in all thermal cycles. The ATFR of B_L ranged between 2.22 °C and 2.45 °C, while that of B_C ranged between 1.91 °C and 2.05 °C. In both bricks, the ATFR showed better thermal performance of the PCM bricks than the bare brick in each thermal cycle since the ATFR values exceeded 0 °C.

The t-Test statistical analysis for the measured inner surface temperature of bricks showed statistical differences, as summarised in Table 4. However, the PCM bricks, B_L and B_C, showed relatively similar standard deviation and standard error of the mean compared with the reference brick, B_R. Besides, the t statistic of PCM bricks was statistically significantly different by more than 2%, which is normal in PCM applications, as indicated by literature studies [32].

3.3. Mechanical test results

Although the current research mainly focuses on the thermal behaviour of constructive concrete bricks when incorporated with PCM, the mechanical strength aspect is significant to show the possibility of incorporating PCM panel/capsules in real applications. In this regard, the bricks were tested for compressive strength (crushing strength test) at 7-day age using a compression testing machine type ADR Touch head from ELE International with a maximum load capacity of 2000 kN. Fig. 11 shows some photos of the machine and test procedure.

The test results showed that the maximum compression strength of B_R, B_L and B_C at the failure was 338.9, 118.1 and 241.7 kN, respectively. These values are equivalent to 12.279, 4.288 and 8.757 N/mm^2 compression strength considering the area of bricks (i.e., 27600 mm^2). As expected, the test result indicated that PCM-integrated bricks had lost their mechanical properties, in which the compression strength of B_L and B_C was reduced by ~65% and ~28.7%, respectively. This strength loosening is mainly attributed to the poor mechanical properties of aluminium containers used for PCM macroencapsulation. It is worth highlighting that the mechanical strength of concrete bricks gives better results at the age of 28 days compared with 7 days. However, the strength of concrete samples at age 7 days is usually above 65% of their strength at 28 days [33]. Therefore, the tested PCM bricks are expected to have a fairly similar mechanical strength difference at age 28 days compared with the reference brick.

4. Discussion

According to the results, the PCM-integrated bricks (i.e., B_L and B_C) generally showed superior thermal performance than the bare brick (B_R). This behaviour is indorsed to the phase change phenomenon, which enhanced the brick's storage inertia and capacity compared to the traditional concrete brick. However, according to the results of Fig. 7, the thermal trend of bricks (including B_R) was reversed around 15:00, and the inner surface temperature was higher than the outer surface temperature. This is anticipated since the bricks were exposed to severe hot weather conditions most day hours with no ventilation for the inside surface, causing heat accumulation on the inner surface. However, the temperature behaviour in real construction cases is expected to differ since direct solar radiation is time-dependent concerning walls. In the late afternoon and nighttime, the temperature behaviour of B_R (considering the T_i and T_o in Fig. 6) was better than that of PCM-integrated bricks, which showed a noticeable temperature difference. This behaviour is endorsed in the solidification/freezing phase of PCM when the stored heat is released from the PCM container(s). However, the temperature behaviour was relatively the same after the midnight of each day cycle (after 00:00 till the beginning of the next cycle), indicating that the PCM was fully solidified in the PCM-integrated bricks, and they started to behave similarly to bare bricks, thermally.

According to the DF results shown in Fig. 8, the performance improvement in the cyclic temperature between the inner and outer surfaces of PCM bricks was minimised, positively improving the indoor temperature in the built environment. The DF of bricks fluctuates daily, depending on the minimum and maximum temperatures of the inner and outer surfaces, which fluctuate following

Table 4
Summary of t-Test statistical analysis applied to the inner surface temperature of bricks.

	B_R	B_L	B_C
Mean	42.178	42.191	41.061
Standard deviation	9.099	8.358	8.449
Standard error of the mean	0.756	0.694	0.702
t statistic	55.817	60.788	58.515

Fig. 11. Compression test (a) brick samples, (b) test machine, (c) B_L under test, (d) display monitor, (e) B_L after test, (f) B_C after test.

outdoor weather conditions. Besides, the DF of PCM bricks is better than the reference brick as long as the PCM melts and solidifies during the thermal cycle. Therefore, the improvement of DF is guaranteed in the following days since the PCM activated in the bricks and the inner surface temperature decreased. The DF results achieved for B_L and B_C by a maximum of 13% and 11% are in good agreement with the PCM applications in the literature. For instance,

These results presented in Fig. 9 regarding the TL, along with the temperature difference results shown in Fig. 7, prove the PCM's ability to shrink and shift the temperature across the bricks. Fig. 9 also shows that the TL fluctuates daily following the outdoor ambient temperatures during the day cycle. Besides, the TL was inconsistent with the daily temperature level, which was lower in the second-day cycle than on the third day, although the latter had lower maximum temperatures, according to Fig. 5. It is worth mentioning that the measurement time step has a certain influence on the TL results in which the lower time steps could generate better resolution of TL values. In other words, the results shown in Fig. 9 could be more realistic if the time step is taken every 1 min instead of the 30 min adopted in this work. This is obviously evidenced in numerical studies, which have more flexibility to evaluate such indicators with a higher range of time steps.

The AFTR difference between the PCM bricks displayed in Fig. 10 was slight, with superior performance for B_L over B_C by about 0.4 °C, 0.3 °C and 0.5 °C on the 1st, 2nd and 3rd day. The ATFR indicator may give a fair evaluation of passive PCM incorporations since it considers the nighttime negative behaviour of PCM along with the thermal behaviour during the day. However, the ATFR results showed a noteworthy indication of the usefulness of PCM in maintaining better thermal management in bricks regardless of the encapsulation configuration.

Overall, all thermal performance evaluation results indicated that the concrete brick integrated with the PCM layer performed slightly better than the one integrated with PCM capsules, although they held the same PCM quantity. This may be attributed to several reasons, including that the encapsulation area of B_L was higher than that of B_C, which enhanced the melting and solidification phases [34]. Furthermore, considering one-dimensional heat flow, the PCM layer can better restrict heat across the brick than the PCM capsules since there will be spaces with no PCM between the capsules. However, increasing the number of thermocouples (more than two) on brick surfaces may obtain closer results. A comparison of the results achieved in the current study compared with similar

Table 5

Summary of literature studies regarding advancements of bricks-based PCM.

Reference	Study location	PCM melting temperature	Brick type	Evaluation indicators/aspects			
				Temperature reduction, °C	DF	TL, h	Other indicators
Gao et al.[35]	Qingdao, China	18–23	Hollow red brick	————	0.92%– 1.93%	5–6	Heat flux reduction by 19.19–21.4 W/m²
Saxena et al. [36]	Delhi, India	36–38	Fired-red clay brick	5–6	————	————	Heat flow reduction by 8%– 12%
Silva et al. [37]	Controlled lab room	18	Hollow red bricks	5	————	3	————
Laaouatni et al.[38]	Lab equipment	27	Hollow concrete block-assisted ventilator	3.4–4.7	————	4.5–6.5	————
Abbas et al. [7]	Diwaniya, Iraq	38–43	Fired-clay hollow brick	4.7	0.7	2	ATFR by 23.84%
Liu et al.[39]	China	44	Foamed cement block	1.45	————	————	————
Chihab et al. [40]	Marrakesh, Morocco	24, 32 and 37	Hollow clay brick	2.48	————	0.7–4.3	Maximum heat flux reduction by 82%
Bachir and Taieb [41]	Bechar, Algeria	32–43	Hollow clay brick	2.5–5.9	————	5.5	Heat flux reduction by 73.7%
Jia et al.[42]	Shanghai, China	20–30	Hollow bricks	1.8–3.4	1.7%– 2.2%	Up to 2.17	Peak heat flow reduction by 19.2–26.1 W/m²
Gupta et al. [43]	Lucknow, India	30.42	Clay brick	0.77–4.2	0.332–0.372	1.2–1.9	Highest heat flux reduction by 33.98%
Current study	Al Amarah, Iraq	40–44	Concrete bricks	5	4.39%	Up to 1.5	ATFR by 1.91–2.45 °C

literature studies can be shown in Table 5.

5. Limitations and insights for future work

The current study highlighted the advancements of concrete bricks when integrated with PCM as a layer or capsules from the thermal and mechanical viewpoints with respect to the bare brick. Some limitations and remarks derived from the current study for further research could be presented as follows:

- The concrete bricks investigated in the current work are fabricated according to the thermal insulation blog provided by the specialised authority in Iraq. However, the shape of bricks is novel since the typical concrete blocks in the country have air cavities to have lighter and thermally better blocks. Therefore, the mechanical strength of the current bricks cannot compare with the normative reference values of typical bricks. This important research theme is open for future works, investigating the influence of PCM and air cavities on the concrete brick's thermal and mechanical behaviour.
- The outcomes generally exhibited that the PCM-integrated layer is slightly superior in enhancing the brick's thermal behaviour compared to the PCM capsules. However, the brick-based PCM layer showed poor mechanical behaviour compared with the one-based PCM capsules. The mechanical strength declination is mainly attributed to the ductility of the container material (aluminium), although it has excellent thermal properties necessary to improve the PCM performance. Accordingly, encapsulation materials of better ductility and thermal characteristics, such as galvanised steel, are recommended for future studies. It is also recommended that such studies be conducted for recycled containers, such as wasted cans, to support the universal concept towards sustainability.
- The current study's findings revealed that the PCM thermal behaviour is affected by changing weather conditions, which had a significant impact on the inner surface temperature of bricks, particularly at night. Therefore, the passive incorporation of PCM should be controlled during the PCM solidification period to ensure full utilisation of the PCM storage capacity throughout the complete thermal cycle. This could be achieved by utilising low temperatures at night with various control strategies. This research area still needs more focus by researchers considering using passive strategies as much as possible.
- The economic evaluation of PCM incorporation is necessary for technology marketing. However, considering the encapsulation material in terms of the material price and encapsulation complexity should be well studied for large wall applications to fairly analyse their influence and which encapsulation method (layer or capsules) is economically feasible.

6. Conclusion

In this study, phase change material (PCM) macroencapsulated into containers was integrated into concrete bricks as a layer (B_L) and capsules (B_C) to investigate their thermal and mechanical performance experimentally. The B_L performed slightly better than the B_C from the thermal point of view, whereas the latter brick was better from the mechanical viewpoint. During the peak day hours,

when the temperature was high and varied considerably, both PCM-integrated concrete bricks outperformed the naked brick in terms of thermal performance. B_L and B_C showed a relatively similar thermal performance to B_R, in which the maximum temperature reduction across the brick reached 5 °C with a time lag of up to 90 min. However, B_L performed slightly better than B_C, considering the decrement factor and average inner surface temperature reduction, reaching a maximum of 4.39% and 0.5 °C, respectively. During the mechanical compression test, both PCM-integrated bricks showed lower mechanical strength than the bare brick, where the compression strength at the failure of B_L and B_C was decreased by ~65% and ~28.7%, respectively. Conclusively, the B_L performed slightly better than B_C thermally, whereas B_C showed superior mechanical properties.

Declaration of Competing Interest

The authors declare that they have no known competing financial interests or personal relationships that could have appeared to influence the work reported in this paper.

Data Availability

Data will be made available on request.

Acknowledgements

References

[1] A.S. Al-Tamimi, O.S. Baghabra Al-Amoudi, M.A. Al-Osta, M.R. Ali, A. Ahmad, Effect of insulation materials and cavity layout on heat transfer of concrete masonry hollow blocks, Constr. Build. Mater. 254 (2020), 119300, https://doi.org/10.1016/j.conbuildmat.2020.119300.

[2] D.S. Vijayan, A. Mohan, J. Revathy, D. Parthiban, R. Varatharajan, Evaluation of the impact of thermal performance on various building bricks and blocks: a review, Environ. Technol. Innov. 23 (2021), 101577, https://doi.org/10.1016/j.eti.2021.101577.

[3] Y. Gao, X. Meng, A comprehensive review of integrating phase change materials in building bricks: methods, performance and applications, J. Energy Storage 62 (2023), 106913, https://doi.org/10.1016/j.est.2023.106913.

[4] M. Arıcı, F. Bilgin, S. Nižetić, H. Karabay, PCM integrated to external building walls: an optimization study on maximum activation of latent heat, Appl. Therm. Eng. 165 (2020), 114560, https://doi.org/10.1016/j.applthermaleng.2019.114560.

[5] A. Chelliah, S. Saboor, A. Ghosh, K.J. Kontoleon, Thermal behaviour analysis and cost-saving opportunities of PCM-integrated terracotta brick buildings, Adv. Civ. Eng. 2021 (2021) 6670930, https://doi.org/10.1155/2021/6670930.

[6] A.C. Rai, Energy performance of phase change materials integrated into brick masonry walls for cooling load management in residential buildings, Build. Environ. 199 (2021), 107930, https://doi.org/10.1016/j.buildenv.2021.107930.

[7] H.M. Abbas, J.M. Jalil, S.T. Ahmed, Experimental and numerical investigation of PCM capsules as insulation materials inserted into a hollow brick wall, Energy Build. 246 (2021), 111127, https://doi.org/10.1016/j.enbuild.2021.111127.

[8] O.J. Imafidon, D.S.-K. Ting, Energy consumption of a building with phase change material walls – the effect of phase change material properties, J. Energy Storage 52 (2022), 105080, https://doi.org/10.1016/j.est.2022.105080.

[9] Z. Liu, J. Hou, Y. Huang, J. Zhang, X. Meng, B.J. Dewancker, Influence of phase change material (PCM) parameters on the thermal performance of lightweight building walls with different thermal resistances, Case Stud. Therm. Eng. 31 (2022), 101844, https://doi.org/10.1016/j.csite.2022.101844.

[10] Z.A. Al-Absi, M.I.M. Hafizal, M. Ismail, H. Awang, A. Al-Shwaiter, Properties of PCM-based composites developed for the exterior finishes of building walls, Case Stud. Constr. Mater. 16 (2022), e00960, https://doi.org/10.1016/j.cscm.2022.e00960.

[11] M. Arıcı, F. Bilgin, M. Krajčík, S. Nižetić, H. Karabay, Energy saving and CO_2 reduction potential of external building walls containing two layers of phase change material, Energy 252 (2022), 124010, https://doi.org/10.1016/j.energy.2022.124010.

[12] S. Shaik, C. Arumugam, S.V. Shaik, M. Arıcı, A. Afzal, Z. Ma, Strategic design of PCM integrated burnt clay bricks: potential for cost-cutting measures for air conditioning and carbon dioxide extenuation, J. Clean. Prod. 375 (2022), 134077, https://doi.org/10.1016/j.jclepro.2022.134077.

[13] R. Saxena, S.F. Ali, D. Rakshit, PCM incorporated bricks: A passive alternative for thermal regulation and energy conservation in buildings for Indian conditions, in: F. Pacheco-Torgal, L. Czarnecki, A.L. Pisello, L.F. Cabeza, C.-G. Granqvist (Eds.), Eco-Efficient Mater. Reducing Cool. Needs Build. Constr, Woodhead Publishing, 2021, pp. 303–328, https://doi.org/10.1016/B978-0-12-820791-8.00014-6.

[14] M. Sam, A. Caggiano, L. Dubyey, J.-L. Dauvergne, E. Koenders, Thermo-physical and mechanical investigation of cementitious composites enhanced with microencapsulated phase change materials for thermal energy storage, Constr. Build. Mater. 340 (2022), 127585, https://doi.org/10.1016/j.conbuildmat.2022.127585.

[15] M.R. Elmarghany, A. Radwan, M.A. Shouman, A.A. Khater, M.S. Salem, O. Abdelrehim, Year-long energy analysis of building brick filled with phase change materials, J. Energy Storage 50 (2022), 104605, https://doi.org/10.1016/j.est.2022.104605.

[16] E. Tunçbilek, M. Arıcı, S. Bouadila, S. Wonorahardjo, Seasonal and annual performance analysis of PCM-integrated building brick under the climatic conditions of Marmara region, J. Therm. Anal. Calorim. 141 (2020) 613–624, https://doi.org/10.1007/s10973-020-09320-8.

[17] C. Ru, G. Li, F. Guo, X. Sun, D. Yu, Z. Chen, Experimental evaluation of the properties of recycled aggregate pavement brick with a composite shaped phase change material, Materials 15 (2022) 5565, https://doi.org/10.3390/ma15165565.

[18] K. Ghasemi, S. Tasnim, S. Mahmud, PCM, nano/microencapsulation and slurries: a review of fundamentals, categories, fabrication, numerical models and applications, Sustain. Energy Technol. Assess. 52 (2022), 102084, https://doi.org/10.1016/j.seta.2022.102084.

[19] Q. Al-Yasiri, M.A. Al- Furaiji, A.K. Alshara, Comparative study of building envelope cooling loads in Al-Amarah city, Iraq, J. Eng. Technol. Sci. 51 (2019) 632–648, https://doi.org/10.5614/j.eng.technol.sci.2019.51.5.3.

[20] Ministry of Construction and Housing- Minstry of Planning,Thermal Insulation Blog (Iraqi Construction Blog), 2013. https://amanatbaghdad.gov.iq/amanarules/pict/مدونات/blog20-الحراري العزل مدونة.pdf.

[21] Q. Al-Yasiri, M. Szabó, Paraffin as a phase change material to improve building performance: an overview of applications and thermal conductivity enhancement techniques, Renew. Energy Environ. Sustain. 6 (2021) 38, https://doi.org/10.1051/rees/2021040.

[22] H.J. Akeiber, M.A. Wahid, H.M. Hussen, A.T. Mohammad, A newly composed paraffin encapsulated prototype roof structure for efficient thermal management in hot climate, Energy 104 (2016) 99–106, https://doi.org/10.1016/j.energy.2016.03.131.

[23] B. Tejedor, E. Lucchi, I. Nardi, Application of Qualitative and Quantitative Infrared Thermography at Urban Level: Potential and Limitations BT - New Technologies in Building and Construction: Towards Sustainable Development, in: D. Bienvenido-Huertas, J. Moyano-Campos (Eds.), New Technol. Build. Constr., Springer Nature Singapore, Singapore, 2022, pp. 3–19, https://doi.org/10.1007/978-981-19-1894-0_1.

[24] P.M. Toure, Y. Dieye, P.M. Gueye, V. Sambou, S. Bodian, S. Tiguampo, Experimental determination of time lag and decrement factor, Case Stud. Constr. Mater. 11 (2019), e00298, https://doi.org/10.1016/j.cscm.2019.e00298.

[25] S. Kenzhekhanov, S.A. Memon, I. Adilkhanova, Quantitative evaluation of thermal performance and energy saving potential of the building integrated with PCM in a subarctic climate, Energy 192 (2020), 116607, https://doi.org/10.1016/j.energy.2019.116607.

[26] Köppen climate classification, (2022). https://www.weatherbase.com/weather/weather-summary.php3?s=56604&cityname=Al+Amarah%2C+Maysan%2C+Iraq&units=.

[27] WeatherSpark, Average hourly temperature, (2022). https://weatherspark.com/y/104342/Average-Weather-in-Al-'Amārah-Iraq-Year-Round#Sections-Temperature.

[28] J. Triano-Juárez, E.V. Macias-Melo, I. Hernández-Pérez, K.M. Aguilar-Castro, J. Xamán, Thermal behavior of a phase change material in a building roof with and without reflective coating in a warm humid zone, J. Build. Eng. 32 (2020), 101648, https://doi.org/10.1016/j.jobe.2020.101648.

[29] Q. Al-Yasiri, M. Szabó, Phase change material coupled building envelope for thermal comfort and energy-saving: effect of natural night ventilation under hot climate, J. Clean. Prod. 365 (2022), 132839, https://doi.org/10.1016/j.jclepro.2022.132839.

[30] P. Arumugam, V. Ramalingam, P. Vellaichamy, Effective PCM, insulation, natural and/or night ventilation techniques to enhance the thermal performance of buildings located in various climates – a review, Energy Build. 258 (2022), 111840, https://doi.org/10.1016/j.enbuild.2022.111840.

[31] P.K.S. Rathore, S.K. Shukla, N.K. Gupta, Yearly analysis of peak temperature, thermal amplitude, time lag and decrement factor of a building envelope in tropical climate, J. Build. Eng. 31 (2020), 101459, https://doi.org/10.1016/j.jobe.2020.101459.

[32] J. Mazo, A.T. El Badry, J. Carreras, M. Delgado, D. Boer, B. Zalba, Uncertainty propagation and sensitivity analysis of thermo-physical properties of phase change materials (PCM) in the energy demand calculations of a test cell with passive latent thermal storage, Appl. Therm. Eng. 90 (2015) 596–608, https://doi.org/10.1016/j.applthermaleng.2015.07.047.

[33] C. Berryman, J. Zhu, W. Jensen, M. Tadros, High-percentage replacement of cement with fly ash for reinforced concrete pipe, Cem. Concr. Res. 35 (2005) 1088–1091, https://doi.org/10.1016/j.cemconres.2004.06.040.

[34] Q. Al-Yasiri, M. Szabó, Effect of encapsulation area on the thermal performance of PCM incorporated concrete bricks: a case study under Iraq summer conditions, Case Stud. Constr. Mater. 15 (2021), e00686, https://doi.org/10.1016/j.cscm.2021.e00686.

[35] Y. Gao, F. He, X. Meng, Z. Wang, M. Zhang, H. Yu, W. Gao, Thermal behavior analysis of hollow bricks filled with phase-change material (PCM), J. Build. Eng. 31 (2020), 101447, https://doi.org/10.1016/j.jobe.2020.101447.

[36] R. Saxena, D. Rakshit, S.C. Kaushik, Phase change material (PCM) incorporated bricks for energy conservation in composite climate: a sustainable building solution, Sol. Energy 183 (2019) 276–284, https://doi.org/10.1016/j.solener.2019.03.035.

[37] T. Silva, R. Vicente, N. Soares, V. Ferreira, Experimental testing and numerical modelling of masonry wall solution with PCM incorporation: a passive construction solution, Energy Build. 49 (2012) 235–245, https://doi.org/10.1016/j.enbuild.2012.02.010.

[38] A. Laaouatni, N. Martaj, R. Bennacer, M. Lachi, M. El Omari, M. El Ganaoui, Thermal building control using active ventilated block integrating phase change material, Energy Build. 187 (2019) 50–63, https://doi.org/10.1016/j.enbuild.2019.01.024.

[39] L. Liu, J. Chen, Y. Qu, T. Xu, H. Wu, G. Huang, X. Zhou, L. Yang, A foamed cement blocks with paraffin/expanded graphite composite phase change solar thermal absorption material, Sol. Energy Mater. Sol. Cells 200 (2019), 110038.

[40] Y. Chihab, R. Bouferra, M. Garoum, M. Essaleh, N. Laaroussi, Thermal inertia and energy efficiency enhancements of hollow clay bricks integrated with phase change materials, J. Build. Eng. 53 (2022), 104569, https://doi.org/10.1016/j.jobe.2022.104569.

[41] A. Bachir, N. Taieb, Numerical analysis for energy performance optimization of hollow bricks for roofing. Case study: hot climate of Algeria, Constr. Build. Mater. 367 (2023), 130336, https://doi.org/10.1016/j.conbuildmat.2023.130336.

[42] C. Jia, X. Geng, F. Liu, Y. Gao, Thermal behavior improvement of hollow sintered bricks integrated with both thermal insulation material (TIM) and phase-change material (PCM), Case Stud. Therm. Eng. 25 (2021), 100938, https://doi.org/10.1016/j.csite.2021.100938.

[43] M.K. Gupta, P.K.S. Rathore, R. Kumar, N.K. Gupta, Experimental analysis of clay bricks incorporated with phase change material for enhanced thermal energy storage in buildings, J. Energy Storage 64 (2023), 107248, https://doi.org/10.1016/j.est.2023.107248.